analytical chemistry

Article

pubs.acs.org/ac

Dual Signaling Molecule Sensor for Rapid Detection of Hydrogen Sulfide Based on Modified Tetraphenylethylene

Wei Zhang, Junqing Kang, Ping Li,* Hui Wang, and Bo Tang*

College of Chemistry, Chemical Engineering and Materials Science, Collaborative Innovation Center of Functionalized Probes for Chemical Imaging in Universities of Shandong, Key Laboratory of Molecular and Nano Probes, Ministry of Education, Shandong Normal University, Jinan 250014, People's Republic of China

Supporting Information

ABSTRACT: A dual signaling molecule sensor has received increasing attention owing to its ability to read out target analytes with more than one transduction channel and thus make the results more convincing. Here we have developed a dual signaling molecule sensor that is well suited for monitoring hydrogen sulfide (H_2S) levels through fluorescence, UV−visible adsorption, and visual mode. Results showed the selective and instantaneous responses of sensor toward intracellular H_2S. Moreover, the sensor was successfully applied to imaging of H_2S levels in *Caenorhabditis elegans* (*C. elegans*) and observed the changes of H_2S under starvation of *C. elegans*. Altogether, the sensor was proved to be a useful tool for tracking H_2S levels in cells and in vivo. The merits of two kinds of independent signaling molecules allow us to select different output modes according to the different samples.

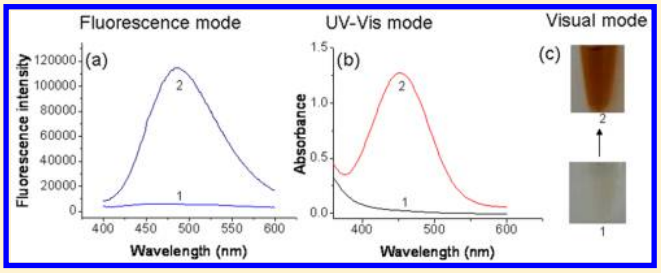

The development of rapid and accurate sensors for H_2S is particularly important, since H_2S is traditionally considered as a toxic gas and recent research has indicated that H_2S, as an important signaling molecule in living organisms, is associated with various physiological processes such as antioxidation, ischemia reperfusion injury, anti-inflammation, and apoptosis.[1−8] The current methods for H_2S detection are most popularly based on electrochemical assays, gas chromatography, and sulfide precipitation;[9−13] although different strategies have been developed, it is still a challenge to implement rapid, facile in situ detection. Therefore, new methods for detection of H_2S are still in high demand.

A dual signaling molecule sensor is of great importance, owing to its ability to read out the target analytes with more than one transduction channel and thus make the results more convincing.[14−18] Currently, most sensors that send out two or more signals are based on the same molecule, which does not allow mutual correction through two kinds of signal to improve the accuracy of the results.[19−26] Importantly, the two kinds of signaling molecules do not interfere with each other. The merits of the sensor are that we can select different output modes according to different samples. However, dual signaling molecule sensors for H_2S, especially for in situ detection in biological samples, are still very limited so far.

Herein, we report a tetraphenylethylene (TPE)-based dual signaling molecule sensor for detection and imaging of H_2S through fluorescence, UV−vis adsorption, and colorimetric mode. As is well-known, TPE, as an aggregation induced emission (AIE) fluorogen, has been used for construction of various fluorescent sensors and successfully applied in the field of biology.[27−31] Recently, Tang and co-workers[32] reported a novel tetraphenylethene-based fluorescent H_2S probe, which exhibited high selectivity and tunable sensitivity, making direct indication of H_2S concentration in blood and unknown samples possible. As shown in Scheme 1, dual signaling molecules can be produced after reaction of the sensor with target analytes: one of the molecules has fluorescent properties, and another molecule produced obvious ultraviolet absorption at 450 nm. The two hydroxyl groups of 4,4′-(1,2-diphenylethene-1,2-diyl)diphenol (TPE-OH) were covalently conjugated with dinitrophenyl ether, which was selected as the H_2S reactive site because of its excellent recognition performance for H_2S. The resultant sensor by itself is nonfluorescent, which was mainly due to electron transfer between TPE-OH and dinitrophenyl ether. However, upon addition of H_2S the sensor showed a strong fluorescence enhancement, accompanied by changes in color and UV absorption. The absorption spectrum at 450 nm from 2,4-dinitrobenzenethiol (DBT, one of the products of the sensor reacted with H_2S). The performance of the sensor was characterized in detail. Furthermore, the selectivity was also evaluated by fluorescent and adsorption experiments and discussed. The as-prepared sensor was successfully applied to imaging of H_2S in cells and observation of changes in H_2S under starvation of *C. elegans*. To the best of our knowledge, dual signaling molecule sensors for H_2S has not been reported to date and are of great significance for the efficient detection of H_2S in biological systems.

Received: June 9, 2015
Accepted: August 3, 2015
Published: August 3, 2015

DOI: 10.1021/acs.analchem.5b02169
Anal. Chem. 2015, 87, 8964−8969

Scheme 1. Proposed Reaction Mechanism[a]

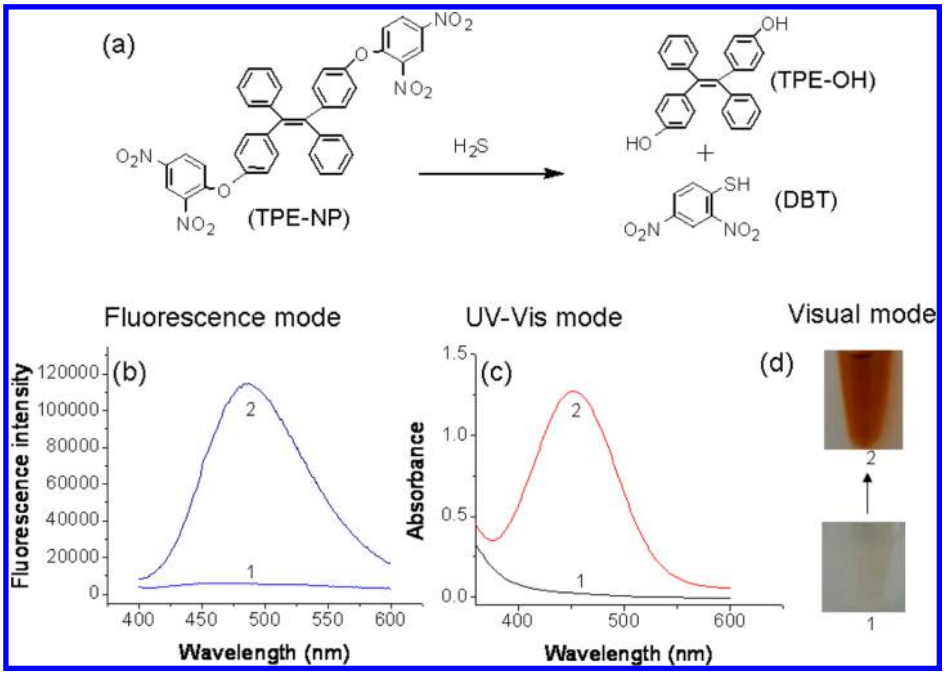

[a](a) Structures of sensor and products. (b) Fluorescence and (c) adsorption spectra of (1) sensor and (2) products. (d) Color changes of solutions of (1) sensor and (2) products.

EXPERIMENTAL SECTION

Materials and Reagents. All chemicals were available commercially, and solvents were purified by conventional methods before use. 4-Hydroxybenzophenone and 1-bromo-2,4-dinitrobenzene were purchased from Sun Chemical Technology Co., Ltd. (Shanghai). Reactive oxygen species were as follows. Hypochlorite (NaOCl), H_2O_2, and *tert*-butylhydroperoxide (TBHP) were delivered from 10%, 30% and 70% aqueous solutions, respectively. Hydroxyl radical ($^{\bullet}OH$) was generated by reaction of 1 mM Fe^{2+} with 200 μM H_2O_2. Nitric oxide (NO) was used from stock solution prepared by sodium nitroprusside. Singlet oxygen ($^1O_2$) was prepared by the ClO^-/H_2O_2 system. Superoxide ($O_2^{\bullet}$) was delivered from KO_2 in dimethyl sulfoxide (DMSO) solution. Peroxynitrite was used from 10 mM stock solution in 0.3 mol/L NaOH.

Instruments. ^1H NMR spectra were recorded with Bruker NMR spectrometer at 300 MHz and JEOL JNM-ECA600. Mass spectra were obtained by Bruker maXis ultra-high-resolution time-of-flight mass spectrometry (TOF MS) system. The fluorescence spectra measurements were performed on a FLS-920 Edinburgh fluorescence spectrometer. Fluorescent images were measured on a Leica TCS SP5 confocal laser scanning microscope with an objective lens (×40). The excitation wavelength was 405 nm (5 mW).

Synthesis of Sensor 1,2-Bis[4-(2,4-dinitrophenoxy)-phenyl]-1,2-diphenylethene. 4,4′-(1,2-Diphenylethene-1,2-diyl)diphenol (TPE-OH) was prepared according to previously published experimental procedures.[33] TPE-OH (0.365 g, 1 mmol), 1-bromine-2,4-dinitrobenzene (0.988 g, 4 mmol), and K_2CO_3 (0.552 g, 4 mmol) were dissolved in anhydrous *N*,*N*-dimethylformamide (DMF) (10 mL). The reaction mixture was then heated at 90 °C for 4.5 h under N_2 atmosphere. After cooling to room temperature, the reaction mixture was poured into ice water (100 mL). The crude product was extracted with ethyl acetate (5 × 25 mL), dried over $MgSO_4$, and purified by flash column chromatography (petroleum ether/CH_2Cl_2 = 1/1) to obtain the compound **2** as a white solid (0.341 g, yield: 49%). ^1H NMR (400 MHz, DMSO) δ 8.883 (s, 2H), 8.520 (d, J = 9.2 Hz, 2H), 7.064−7.246 (m, 20H; ArH). ^{13}C NMR (100 MHz, DMSO) δ 142.96, 141.87, 141.50, 140.65, 139.82, 133.36, 131.19, 130.14, 128.55, 127.46, 122.37, 120.57, 119.38. MS data, m/z 697.1526 (M + H). Melting point 224.5 °C.

Cell and Worm Culture. HeLa cells were cultured in Dulbecco's modified Eagle medium (DMEM) containing 10% fetal bovine serum (FBS), 1% penicillin, and 1% streptomycin at 37 °C (w/v) in a 5% CO_2/95% air incubator, model MCO-15AC (Sanyo, Tokyo, Japan). The concentrations of counted cells were adjusted to 1 × 10^6 cells·mL^{-1} for confocal imaging in high-glucose DMEM (4.5 g of glucose/L) supplemented with 10% FBS, $NaHCO_3$ (2 ng/L), and 1% antibiotics (penicillin/streptomycin, 100 units/mL). Cultures were maintained at 37 °C under a humidified atmosphere containing 5% CO_2.

C. elegans were cultured at 20 °C on solid nematode growth medium (NGM) with *Escherichia coli* strain OP50. Eggs were placed on the plates (100−200 eggs/plate) and left to hatch and grow to the beginning of the adult stage. Worms were moved to new assay plates every 2 days, until all the worms on the plate laid no more eggs. Then the worms were divided into two plates, with or without OP50.

Confocal Imaging. Fluorescent images were acquired on a Leica TCS SP5 confocal laser scanning microscope with an objective lens (×40). The excitation wavelengths were 405 nm (5 mW) and 488 nm (15 mW). Following incubation, the cells were washed three times in DMEM without FBS and imaged. *C. elegans* were imaged directly after incubation.

DOI: 10.1021/acs.analchem.5b02169
Anal. Chem. 2015, 87, 8964−8969

RESULTS AND DISCUSSION

The dual signaling molecule sensor TPE-NP, as shown in Scheme S1 in Supporting Information, consists of TPE and dinitrophenyl ether. TPE-NP was characterized by ^{1}H NMR, ^{13}C NMR, and MS, and structures of the products (TPE-OH and DBT) were confirmed by MS. Fluorescence and absorption properties of TPE-NP were tested in aqueous solution [0.015 M *N*-(2-hydroxyethyl)piperazine-*N*′-ethanesulfonic acid (HEPES) in tetrahydrofuran (THF)/water = 1:9 (v/v), pH 7.4]. TPE-NP exhibited no fluorescence emission; when H_2S was added to the solution of TPE-NP, the fluorescence emission band centered at 480 nm was enhanced significantly. Moreover, TPE-NP exhibited no absorption features in the visible region (450 nm) and the solution of TPE-NP was colorless (Scheme 1d and Figure 1). When H_2S was added to the solution of TPE-NP, a new absorption band centered at 450 nm developed quickly (Scheme 1c), which induced a change from colorless to brown (Scheme 1d). By color change, we can distinguish various concentrations of H_2S by direct observation with the eyes. From Figure 1, the lowest concentration that we can distinguish reached nanomolar level. Through the experiment of UV−vis, there was good linearity between absorbance and concentrations of H_2S in the range of 0.1 μmol−0.8 mmol/L, with a detection limit of 12.8 nmol/L. The time-dependent fluorescence responses were next detected. After addition of H_2S, a pronounced fluorescence increase and color change was obtained instantly (Figure S1). Notably, the background fluorescence of TPE-NP is very weak, and within a few seconds a high fluorescence increase is observed. Therefore, the time scale allows TPE-NP to sense H_2S in real-time intracellular imaging. The effect of pH on fluorescence and adsorption of TPE-NP was also evaluated, and the results are shown in Figures S2 and S3. It can be seen that TPE-NP exhibit good performance at around pH 7.4 and identical results of fluorescence and UV−vis absorption were obtained, and the cross-referencing experiments make the test results more credible. Thus, the sensor was expected to work well under physiological conditions.

Figure 1. Color changes of solutions of sensor and various concentrations of analyte as observed by the naked eye: (sample 1) control; (samples 2−7) 10^{-9}, 10^{-8}, 10^{-6}, 10^{-5}, 10^{-4}, and 10^{-3} mol/L, respectively.

Selectivity of fluorescence and UV−vis adsorption responses of TPE-NP to H_2S was then examined. Figure 2 shows fluorescence and absorbance responses of TPE-NP to various anions and sulfur-containing analytes in aqueous solutions (THF/water = 1:9, pH 7.4). Selective and large fluorescent and absorbance enhancements were observed upon addition of H_2S to the solution of TPE-NP. Addition of 100 equiv of I^-, Cl^-, Br^-, etc., even at higher concentrations than H_2S, did not lead to significant fluorescence and absorbance responses with TPE-NP under the same conditions, which showed its high selectivity toward H_2S. The results for fluorescence were consistent with those for absorbance, and these identical phenomena make the results more convincible.

TPE-NP is nonfluorescent in either solution or solid state, and the fluorescence of TPE-NP is probably quenched by the NP unit associated with electronic effect. After the sensor reacted with H_2S, fluorescence emission at 480 nm should belong to TPE-OH, which resulted from thiolysis of the dinitrophenyl ether by H_2S. To verify this mechanism, the reaction products of TPE-NP with H_2S were analyzed by HPLC with UV and fluorescence detectors, respectively (Figure 3). As shown in Figure 3a, only one absorption peak for TPE-NP was observed. After TPE-NP reacted with H_2S, two absorption peaks for products can be found, because two reaction products weregenerated when TPE-NP reacted with H_2S. Results from the fluorescence detector further proved this mechanism. It can be seen from Figure 3b that TPE-NP is nonfluorescent, and fluorescence emission is due to TPE-OH, which indicates that the NP unit is responsible for the quenching in the TPE-NP sensor.

We next tested the ability of TPE-NP to be used to visualize H_2S in live cells. HeLa cells were incubated with TPE-NP and exhibited no fluorescence (Figure S5). Then the cells were incubated with 50 mmol/L H_2S, a concentration comparable with physiological H_2S levels, and they displayed enhanced

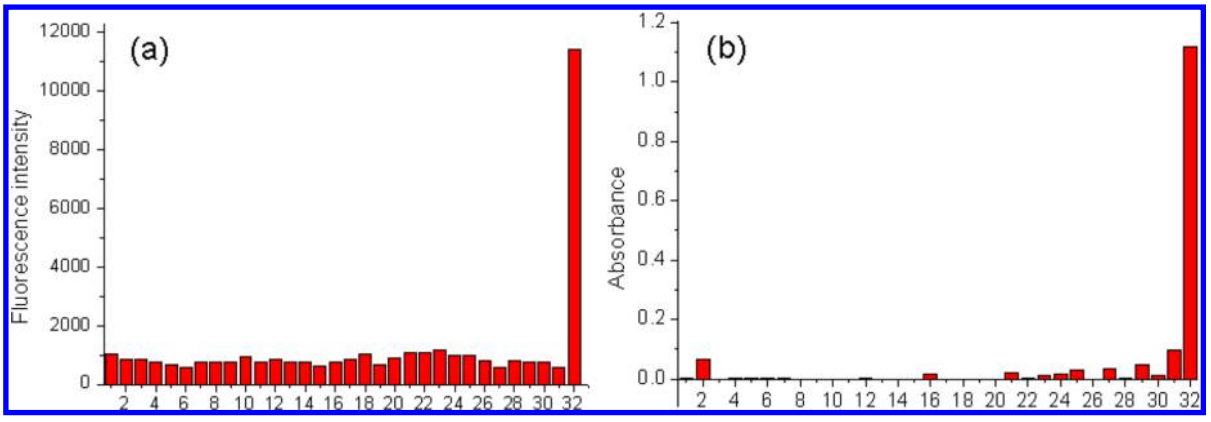

Figure 2. (a) Fluorescence and (b) absorbance responses of 10 mmol/L TPE-NP to various analytes in aqueous solution: (1) control, (2) I^-, (3) Br^-, (4) Cl^-, (5) CO_3^{2-}, (6) HCO_3^-, (7) $H_2PO_4^-$, (8) HPO_4^{2-}, (9) NO_3^-, (10) VC, (11) Zn^{2+}, (12) Mg^{2+}, (13) K^+, (14) Ca^{2+}, (15) Ac^-, (16) $S_2O_3^{2-}$, (17) $S_2O_4^{2-}$, (18) $S_2O_5^{2-}$, (19) SO_3^{2-}, (20) SO_4^{2-}, (21) ButOOH, (22) ClO^-, (23) H_2O_2, (24) NO, (25) O_1, (26) O_2, (27) OH^-, (28) $ONOO^-$, (29) GSH, (30) HCY, (31) S^{2-}, and (32) HS^-.

DOI: 10.1021/acs.analchem.5b02169
Anal. Chem. 2015, 87, 8964−8969

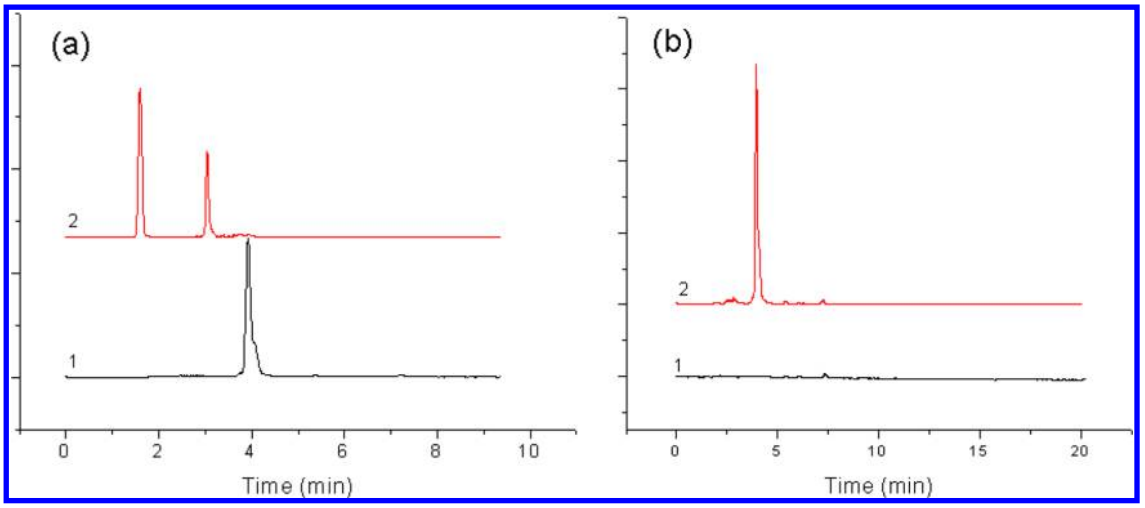

Figure 3. (a) HPLC with UV detector. Spectrum 1, TPE-NP; spectrum 2, reaction products of TPE-NP with H_2S. (b) HPLC with fluorescence detector. Spectrum 1, TPE-NP; spectrum 2, reaction products of TPE-NP with H_2S. HPLC on an octadecylsilica (ODS) column was monitored at 230 nm (a, UV detector) or 400 nm (b, fluorescence detector). Experimental conditions: column, 250 mm × 4.6 mm i.d.; mobile phase, methanol; flow rate, 0.8 mL/min.

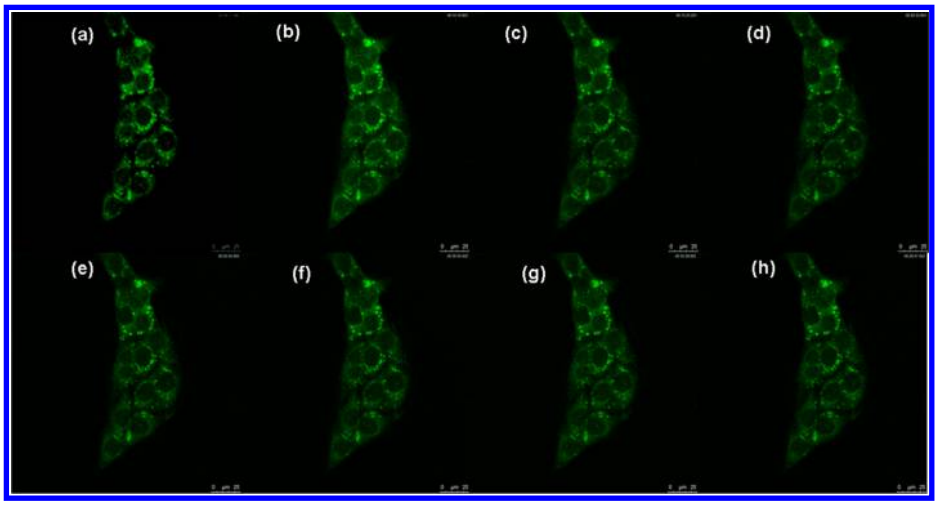

Figure 4. Fluorescence images of living mouse macrophages from the sensor TPE-NP at different time intervals. Images were acquired with 400 nm excitation: (a–h) 0, 10, 20, 30, 40, 50, 60, and 80 min, respectively.

green fluorescence (Figure S5). In contrast, appropriate fluorescence was observed after treatment with sodium nitroferricyanide(III) dehydrate (SNP), which indicated that TPE-NP could visualize the changes of H_2S levels in cells. Moreover, the cytotoxicity of TPE-NP was examined toward HeLa cells by a 3-(4,5-dimethylthiazol-2-yl)-2,5-diphenyltetrazolium bromide (MTT) assay (Figure S6). The results showed that 95% of HeLa cells survived after 12 h, demonstrating that TPE-NP was of low toxicity toward the corresponding cells. These experiments demonstrate that TPE-NP can be employed as a fluorescent sensor to image H_2S in living cells.

Compared with the traditional dye, the TPE-based sensor has better resistance to photobleaching.[26,34] To illustrate this advantage of the TPE-based sensor, we observed the fluorescent intensity in 80 min upon irradiation (five times/min), and the results are shown in Figure 4. It can be seen that the fluorescence of the living cells emits intensely at the first passage and the fluorescence intensity of the stained cells does not change much, which indicate that TPE-NP can serve as fluorescent bioprobes for long-term cell tracing.

In order to exhibit the applications of TPE-NP in intravital imaging, fluorescent imaging of H_2S in *C. elegans* was then performed. As shown in Figure 5, strong fluorescence was observed when the sensor-loaded *C. elegans* were treated with SNP (Figure 5c), and much stronger fluorescence was observed after addition of H_2S (Figure 5e), which showed the good performance of the sensor for imaging of H_2S levels in vivo.

With the aim of further verifying the performance of the sensor, the resultant sensor was then applied to observed levels of H_2S of *C. elegans* under starvation. The H_2S in *C. elegans* was generated under starvation, and the levels of H_2S will rise with time. Figure 6 shows the results of H_2S levels over 3 days. Panels a (control) and b (incubated with sensor) show results from the first day; the levels of H_2S of *C. elegans* increased significantly. The same results were observed on the second and third days. The level of H_2S on the third day was obviously higher than that of the first 2 days. Those results indicated the sensor was an ideal tool to further investigate H_2S in vivo.

Finally, the developed sensor TPE-NP was employed for selective detection of H_2S in the environment. Appropriate solutions from Heihu Spring, Wulong Lake, and Daming Lake

DOI: 10.1021/acs.analchem.5b02169
Anal. Chem. 2015, 87, 8964–8969

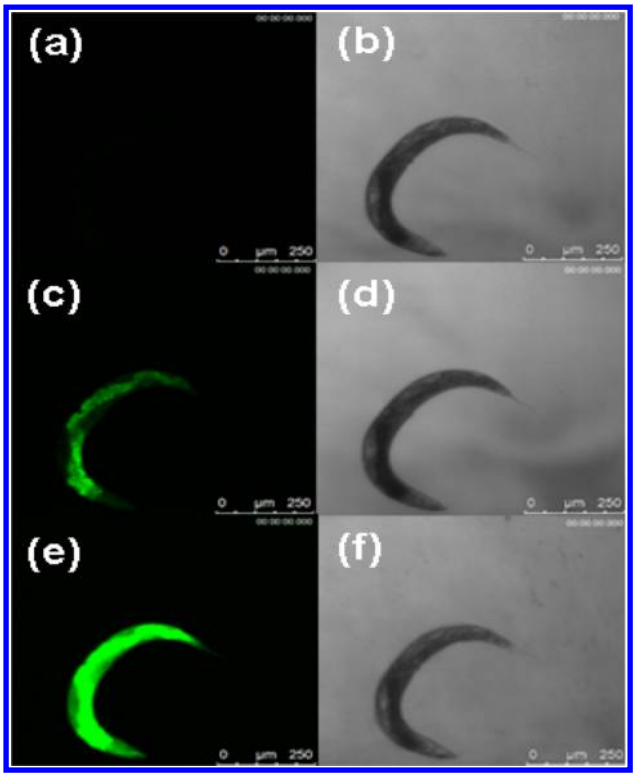

Figure 5. Fluorescence images of H_2S: (a) sensor-loaded *C. elegans*, (c) sensor for H_2S under stimulation with SNP, and (e) sensor-loaded zebrafish stimulated with H_2S. Panels b, d, and f are bright-field images of panels a, c, and e, respectively.

locations spiked with H_2S were found to be sufficient for quantitative recovery of H_2S (Table 1).

CONCLUSIONS

In summary, we have developed a dual signaling molecule sensor for detection and imaging of H_2S through changes of fluorescence, UV−vis absorption, and visual mode. By color change, we can rapidly distinguish various levels of H_2S by direct observation with the eyes. The lowest concentration that we could distinguish was nanomolar level. In addition, the sensor was used for monitoring intracellular H_2S levels selectively. Finally, the sensor as a fluorescent imaging tool was well-suited for tracking H_2S levels in *C. elegans* and allowed us to observe changes of H_2S under starvation of *C. elegans*. The features of the dual signaling molecule sensor make it an ideal tool to further investigate H_2S levels in biological processes and in the environment quickly and easily. By use of different samples to select the appropriate output mode, we can not only expand the application range of the sensor but also make full use of the characteristics of the sensor to improve sensitivity of detection.

Table 1. Results for Determination of H_2S in Different Samples

	H_2S concn ($\times 10^{-6}$ M)		
sample	spiked	measured[a]	%[a]
Heihu Spring	0.0	nd[b]	
Heihu Spring	1.0	1.06 ± 0.01	106.0 ± 1.0
Wulong Lake	0.0	nd[b]	
Wulong Lake	1.0	1.06 ± 0.02	106.0 ± 2.0
Daming Lake	0.0	nd[b]	
Daming Lake	2.0	1.96 ± 0.08	97.6 ± 4.0

[a]Mean ± std, n = 3; mean ± std recovery, %. [b]Not detected.

ASSOCIATED CONTENT

Supporting Information

The Supporting Information is available free of charge on the ACS Publications website at DOI: 10.1021/acs.analchem.5b02169.

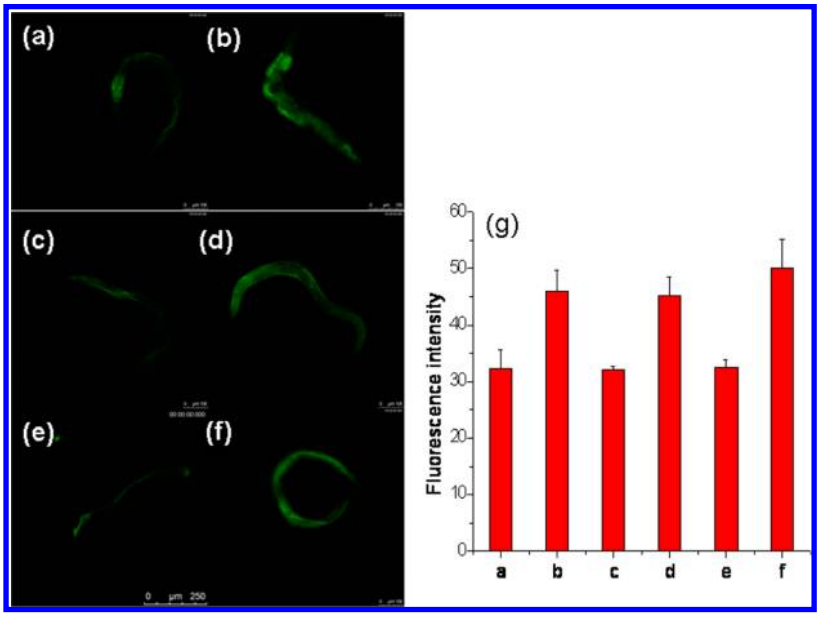

Figure 6. Fluorescence images of H_2S in *C. elegans*. Panels a, c, and e show controls on days 1, 2, and 3, respectively. Panels b, d, and f show fluorescent images of sensor-loaded *C. elegans* under starvation on days 1, 2, and 3, respectively. (g) Fluorescence intensity output from the fluorescent images (panels a−f).

DOI: 10.1021/acs.analchem.5b02169
Anal. Chem. 2015, 87, 8964−8969

Synthesis of TPE-NP sensor, fluorescence kinetic response of sensor to H_2S, effect of different kinds of buffer solution, conditions optimization, fluorescence and absorption spectra, fluorescence images and viability of HeLa cells, and ^{13}C NMR, ^{1}H NMR, and mass spectra (PDF)

AUTHOR INFORMATION

Corresponding Authors

*E-mail: lip@sdnu.edu.cn.
*E-mail tangb@sdnu.edu.cn.

Notes

The authors declare no competing financial interest.

ACKNOWLEDGMENTS

This work was supported by 973 Program (2013CB933800), National Natural Science Foundation of China (21227005, 21390411 and 21305080), Natural Science Foundation of Shandong Province of China (ZR2015JL008 and ZR2013BQ005), and Program for Changjiang Scholars and Innovative Research Team in University.

REFERENCES

(1) Culotta, E.; Koshland, D. E. *Science* **1992**, *258*, 1862−1865.
(2) Morita, T.; Perrella, M. A.; Lee, M. E.; Kourembanas, S. *Proc. Natl. Acad. Sci. U. S. A.* **1995**, *92*, 1475−1479.
(3) Szabó, C. *Nat. Rev. Drug Discovery* **2007**, *6*, 917−935.
(4) Liu, C.; Pan, J.; Li, S.; Zhao, Y.; Wu, L. Y.; Berkman, C. E.; Whorton, A. R.; Xian, M. *Angew. Chem., Int. Ed.* **2011**, *50*, 10327−10329.
(5) Lefer, D. J. *Proc. Natl. Acad. Sci. U. S. A.* **2007**, *104*, 17907−17908.
(6) Eto, K.; Asada, T.; Arima, K.; Makifuchi, T.; Kimura, H. *Biochem. Biophys. Res. Commun.* **2002**, *293*, 1485−1488.
(7) Liu, J.; Sun, Y.; Zhang, J.; Yang, T.; Cao, J.; Zhang, L.; Guo, W. *Chem. - Eur. J.* **2013**, *19*, 4717−4722.
(8) Huang, Z.; Ding, S.; Yu, D.; Huang, F.; Feng, G. *Chem. Commun.* **2014**, *50*, 9185−9187.
(9) Han, Y.; Qin, J.; Chang, X.; Yang, Z.; Du, Z. *Cell. Mol. Neurobiol.* **2006**, *26*, 101−107.
(10) Ubuka, T. *J. Chromatogr. B: Anal. Technol. Biomed. Life Sci.* **2002**, *781*, 227−249.
(11) Tangerman, A. *J. Chromatogr. B: Anal. Technol. Biomed. Life Sci.* **2009**, *877*, 3366−3377.
(12) Doeller, J. E.; Isbell, T. S.; Benavides, G.; Koenitzer, J.; Patel, H.; Patel, R. P.; Lancaster, J. R., Jr.; Darley-Usmar, V. M.; Kraus, D. W. *Anal. Biochem.* **2005**, *341*, 40−51.
(13) Nagata, T.; Kage, S.; Kimura, K.; Kudo, K.; Noda, M. *J. Forensic Sci.* **1990**, *35*, 706−712.
(14) Wu, P.; Miao, L.; Wang, H.; Shao, X.; Yan, X. *Angew. Chem., Int. Ed.* **2011**, *50*, 8118−8121.
(15) Schmittel, M.; Lin, H. W. *Angew. Chem., Int. Ed.* **2007**, *46*, 893−896.
(16) Liu, D.; Liu, M. Y.; Liu, G. H.; Zhang, S. C.; Wu, Y. Y.; Zhang, X. R. *Anal. Chem.* **2010**, *82*, 66−68.
(17) Hierlemann, A.; Gutierrez-Osuna, R. *Chem. Rev.* **2008**, *108*, 563−613.
(18) Hagleitner, C.; Hierlemann, A.; Lange, D.; Kummer, A.; Kerness, N.; Brand, O.; Baltes, H. *Nature* **2001**, *414*, 293−296.
(19) Gutierrez-Osuna, R.; Hierlemann, A. *Annu. Rev. Anal. Chem.* **2010**, *3*, 255−276.
(20) Rusin, O.; St. Luce, N. N.; Agbaria, R. A.; Escobedo, J. O.; Jiang, S.; Warner, I. M.; Dawan, F. B.; Lian, K.; Strongin, R. M. *J. Am. Chem. Soc.* **2004**, *126*, 438−439.
(21) Wang, X.; Sun, J.; Zhang, W.; Ma, X.; Lv, J.; Tang, B. *Chem. Sci.* **2013**, *4*, 2551−2556.
(22) He, M.; Johnson, R.; Escobedo, J. O.; Beck, J. A.; Kim, K. K.; St. Luce, N. N.; Davis, C. J.; Lewis, P. T.; Fronczek, F. R.; Melancon, B. J.; Mrse, A. A.; Treleaven, W. D.; Strongin, R. M. *J. Am. Chem. Soc.* **2002**, *124*, 5000−5009.
(23) Chen, Y.; Zhu, C.; Yang, Z.; Chen, J.; He, Y.; Jiao, Y.; He, W.; Qiu, L.; Cen, J.; Guo, Z. *Angew. Chem., Int. Ed.* **2013**, *52*, 1688−1691.
(24) Wang, Y.; Zhang, Y.; Wu, X.; He, X.; Li, W. *Mater. Lett.* **2015**, *143*, 326−329.
(25) Peng, H.; Cheng, Y.; Dai, C.; King, A. L.; Predmore, B. L.; Lefer, D. J.; Wang, B. *Angew. Chem., Int. Ed.* **2011**, *50*, 9672−9675.
(26) Wang, S.; Li, N.; Pan, W.; Tang, B. *TrAC, Trends Anal. Chem.* **2012**, *39*, 3−37.
(27) Ding, D.; Li, K.; Liu, B.; Tang, B. Z. *Acc. Chem. Res.* **2013**, *46*, 2441−2453.
(28) Hong, Y.; Lam, J. W. Y.; Tang, B. Z. *Chem. Soc. Rev.* **2011**, *40*, 5361−5388.
(29) Wang, Z.; Chen, S.; Lam, J. W. Y.; Qin, W.; Kwok, R. T. K.; Xie, N.; Hu, Q.; Tang, B. Z. *J. Am. Chem. Soc.* **2013**, *135*, 8238−8245.
(30) Hu, F.; Huang, Y.; Zhang, G.; Zhao, R.; Zhang, D. *Tetrahedron Lett.* **2014**, *55*, 1471−1474.
(31) Yuan, Y.; Kwok, R.; Tang, B. Z.; Liu, B. *J. Am. Chem. Soc.* **2014**, *136*, 2546−2554.
(32) Cai, Y.; Li, L.; Wang, Z.; Sun, J. Z.; Qin, A.; Tang, B. Z. *Chem. Commun.* **2014**, *50*, 8892−8895.
(33) Zhao, Q.; Li, K.; Chen, S.; Qin, A.; Ding, D.; Zhang, S.; Liu, Y.; Liu, B.; Sun, J. Z.; Tang, B. Z. *J. Mater. Chem.* **2012**, *22*, 15128−15135.
(34) Wang, Z.; Chen, S.; Lam, J. W. Y.; Qin, W.; Kwok, R. T. K.; Xie, N.; Hu, Q.; Tang, B. Z. *J. Am. Chem. Soc.* **2013**, *135*, 8238−8245.

DOI: 10.1021/acs.analchem.5b02169
Anal. Chem. 2015, 87, 8964−8969